Megawatt Isobaric Compressed Air Energy Storage: an Experimental Study on the Discharge Process[#]

Changchun Liu[1, 2, 3], Zhao Yin[1, 2], Xu Su[3], Xuehui Zhang[1, 2], Zhitao Zuo[1, 2], Yong Sheng[1, 2], Xuezhi Zhou[1, 2], Xudong Wang[4], Yujie Xu[1, 2, *], Haisheng Chen[1, 2, *]

1 Institute of Engineering Thermophysics, Chinese Academy of Sciences, Beijing 100190, China
2 University of Chinese Academy of Sciences, Beijing 100049, China
3 Nanjing Institute of Future Energy System, Institute of Engineering Thermophysics, Chinese Academy of Sciences, Nanjing, 211135, China
4 Institute of Systems Engineering, Academy of Military Sciences, Beijing 102300, China
(Corresponding Author: xuyujie@iet.cn/chen_hs@iet.cn)

ABSTRACT

Isobaric compressed air energy storage is a pivotal technology enabling the extensive deployment of renewable energy in coastal regions. Recently, there has been a surge in research integrating isobaric compressed air energy storage with various renewables. However, there remains a significant shortage of experimental verifications. This paper presents an experimental study on the discharge process of a megawatt isobaric compressed air energy storage system, revealing the regulation characteristics of the start-up, isobaric discharge operation, and shut-down processes. Experiments show that the energy storage system has reliable and rapid regulation characteristics, with vibration less than 41um, cold start time not exceeding 5 min, and shut down within 2 min. The storage system with a flexible storage device can fully utilize the stored compressed air while maintaining stable pressure at the compressor outlet and turbine inlet. The findings of this study lay the foundation for the actual application of isobaric compressed air energy storage systems in the development and utilization of renewable energy along coastal areas.

Keywords: Isobaric compressed air energy storage; Underwater compressed air energy storage; Constant pressure energy storage; Experimental investigation.

NOMENCLATURE

Abbreviations	
CAES	Compressed air energy storage
NIST	National Institute of Standards and Technology
UWCAES	Underwater CAES

Symbols	
m	Air mass flow rate
n	Speed
P	Pressure
T	Temperature
T_q	Torque
V	Volumetric flow rate
W_t	Shaft power
ρ	Density

1. INTRODUCTION

According to the International Energy Agency, more than 500 gigawatts of renewable generation capacity are set to be added in 2023, setting a new record. Renewables such as wind, solar, and wave power are known for their intermittency, instability, and unpredictability. Connecting these renewables to the grid can result in various challenges, including voltage instability [1], increased oscillations [2], reduced inertia [3], and channel congestion. Integrating uncontrollable renewables like wind and solar power exacerbates the volatility and instability of the power system [4]. As the scale of wind and solar power continues to increase, there is an anticipated rise in the demand for long-duration and large-scale energy storage solutions in the future [5].

Existing electrical energy storage technologies encompass pumped hydro storage [6], compressed air energy storage [7], batteries [8], superconductors [9], flywheels [10], and capacitors [11]. Each of these storage methods exhibits distinct performance characteristics and is suitable for various applications and domains. However, only pumped hydro storage and compressed air energy storage (CAES) concurrently demonstrate

advantages in terms of scale, longevity, and cost-effectiveness [12]. Currently, pumped hydro storage is the predominant technology used for large-scale energy storage in China. Despite its maturity, pumped hydro faces natural geographical constraints [13], particularly due to mismatches with the distribution of wind and solar resources in China [14]. Additionally, its capacity and functionality cannot fully meet the growing energy storage needs. Hence, there is a clear imperative to develop alternative large-scale energy storage technologies beyond pumped hydro. CAES is highly regarded for its substantial storage capacity, long storage duration, and relatively lower investment costs. Consequently, it is regarded as the most promising large-scale energy storage technology with vast development prospects [15]. Despite its initial foray into commercial development, effectively integrating CAES into coastal renewable energy scenarios remains an unresolved challenge. Coastal regions, characterized by spatial limitations and operating independently from the primary grid, demand exploring innovative energy storage technologies tailored to their specific environmental conditions [16].

Underwater CAES (UWCAES), also known as isobaric CAES, holds natural development advantages in coastal environments [17]. This technology involves placing air storage facilities underwater, utilizing the hydrostatic pressure of water for compressed air storage and release [18]. This configuration ensures consistent pressure at the compressor outlet and expander inlet, keeping the compressor and expander operating near their rated conditions. This significantly enhances system efficiency and stability compared to isochoric CAES systems [19]. With the storage facilities located underwater, the system requires minimal land area and offers high levels of safety [20]. Additionally, during operation, the system does not require the maintenance of a minimum air pressure in the storage device. This allows for complete air release and maximizes the utilization of storage devices, resulting in a significantly higher energy density compared to isochoric CAES systems [16]. In 1997, the University of California, San Diego proposed the use of rigid containers for UWCAES. In 2007, the University of Nottingham in the UK conducted initial indoor pool tests followed by underwater trials at the seaside [21]. Hydrostor in Canada and the University of Windsor have conducted significant engineering demonstrations and research in UWCAES [22]. In 2009, Hydrostor conducted the first UWCAES test at a depth of 18 meters. Subsequently, in 2017, they implemented the first onshore UWCAES system demonstration in Lake Ontario,

Canada. The system utilized six air storage bags fixed to the seabed 65 meters below the water surface, with a generating capacity of 660 kW, making it the only demonstrated UWCAES system internationally [23]. Neu et al. [24] experimentally explored heat transfer during the liquid piston compression process in a near-isothermal UWCAES system. Their findings suggest that enhancing heat exchange is achievable by increasing the length of the compression chamber or decreasing the speed of the liquid piston. Subsequently, an experiment on internal airflow in the slow piston compressor of an isothermal CAES system followed soon after [25].

Existing experimental research on CAES systems mainly focuses on key components like compressors, expanders, thermal storage heat exchangers, and air storage vessels. There is limited experimental literature on the overall system of CAES, with a predominant focus on isothermal CAES systems. Experimental inquiries into isobaric CAES systems, particularly megawatt-scale isobaric CAES systems with thermal storage, have not been undertaken. This study marks the first attempt at experimental research on megawatt-scale thermal storage isobaric CAES, revealing the regulation characteristics during start-up, operation, and shutdown of the isobaric energy discharge process. These findings establish the groundwork for the practical application of isobaric CAES systems.

2. EXPERIMENTAL SYSTEM

The layout of the isobaric CAES experimental prototype is presented in Fig. 1. The experimental prototype consists of a middle-pressure four-stage piston compressor, a high-pressure two-stage piston compressor, a high-pressure storage tank with a volume of 30 m^3, an isobaric storage device with a volume of 28 m^3, a four-stage centripetal turbine, a hydraulic dynamometer, an eddy current dynamometer and four heaters.

Due to the challenges posed by geographical constraints and the high costs associated with conducting experiments directly underwater, an isobaric storage device is utilized. This device comprises a sizable storage tank along with a flexible airbag, facilitating the achievement of the isobaric air discharge process. The storage tank is used to uphold a consistent external pressure on the airbag, emulating the static pressure underwater. Throughout the energy release process, the compressed air in the storage tank is consistently replenished by the high-pressure storage tank. The compressed air is discharged from the airbag and directed into the turbine for expansion after undergoing

heating by the heater. The shaft power of the turbine is determined through a collaborative effort involving the series eddy current dynamometer and the hydraulic dynamometer. The eddy current dynamometer offers high sensitivity and rapid response capabilities, while the hydraulic dynamometer possesses high power and slower response characteristics. Consequently, the eddy current dynamometer is initially utilized to stabilize the speed during the start-up process, after which the hydraulic dynamometer is engaged to share the load.
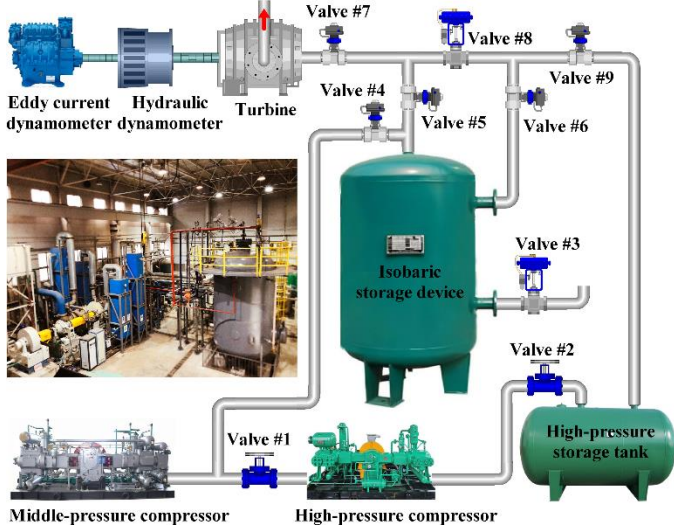
Fig. 1 Layout of the experimental prototype

3. METHODOLOGY

3.1 Operation strategies

Initially, the isobaric storage device is pressurized with compressed air to around 7 MPa using the mid-pressure compressor (Valve #1, #3, #5 and #6 closed, Valve #4 open), with the heat from compression being stored in a hot water tank. Subsequently, the high-pressure tank is pressurized to 27 MPa through a collaborative compression process involving both the middle-pressure compressor and the high-pressure compressor (Valve #4 and #9 closed, Valve #1 and #2 open). The discharge process encompasses several stages, comprising the startup phase, isobaric discharge, and shutdown. Throughout this process, stored hot water is utilized to reheat the air at each turbine stage inlet. Considering the limited volume of the isobaric storage device and the similarity between the startup/shutdown processes of isobaric discharge and isochoric discharge, the compressed air from the high-pressure storage tank is used to explore the startup/shutdown characteristics of the discharge process.

The startup process (Valve #2, #4, #5 and #6 closed, Valve #7, #8 and #9 open) comprises three stages: low-speed rotation to ensure unit normalcy, traversing the critical speed range, and elevation to the rated speed and load. Upon reaching the rated speed and load, the gas source undergoes a switch (Valve #2, #4 and #8 closed, Valve #5, #6, #7 and #9 open). The isobaric storage device provides compressed air to the turbine, while the compressed air from the high-pressure storage tank replenishes the isobaric storage device to sustain a consistent external pressure on the airbag. During the shutdown process, the compressed air source shifts back to the high-pressure storage tank (Valve #8 open, Valve #5 and #6 closed). Subsequently, the turbine intake pressure gradually decreases until it reaches atmospheric pressure, causing the turbine rotation to cease completely.

3.2 Data processing

The data collected during the experiment are all in steady-state conditions. Given the substantial range of pressure changes and the notable deviation of gas properties from ideal gas behaviour, the physical parameters of air are determined by referring to the National Institute of Standards and Technology (NIST) database REFPROP. After the data processing, the following parameters can be obtained:

(1) Mass flow

The mass flow rate of the turbine is calculated using the measured volumetric flow rate, air pressure and air temperature:

$$m = V \cdot \rho_{(P,T)}$$

where m refers to the mass flow rate. V is the measured volumetric flow rate. ρ donates the density at the flow rate measurement point, which is determined by referring to the REFPROP with air pressure and temperature. P and T represent the air pressure and temperature at the flow rate measurement point.

(2) Shaft power

The shaft power of the centripetal turbine is absorbed by two dynamometers. The shaft power of the dynamometer can be determined by measuring torque and speed.

$$W_t = T_q \cdot \frac{2\pi n}{60}$$

where W_t refers to shaft power, T_q represents torque, and n is speed.

4. RESULTS AND ANALYSIS

The results of the isobaric energy discharge experiment are presented and analyzed in this section. The temperature, pressure, and air mass flow discharge

of the isobaric air storage device are illustrated in Fig. 2. Unlike isochoric CAES, where the compressed air pressure and temperature within the storage device decrease continuously, the pressure and temperature within the gas storage device of isobaric CAES remain nearly constant throughout the entire energy discharge experimental process. Specifically, the average temperature and pressure inside the gas storage device are 20.01 °C and 7.05 MPa, respectively. At 16:39, the turbine air source was switched to the flexible gas storage device. The entire switching process lasted less than 20 seconds, and following the switch, the flow rate remained stable at 4.5 kg/s until the compressed air within the airbag was completely released.
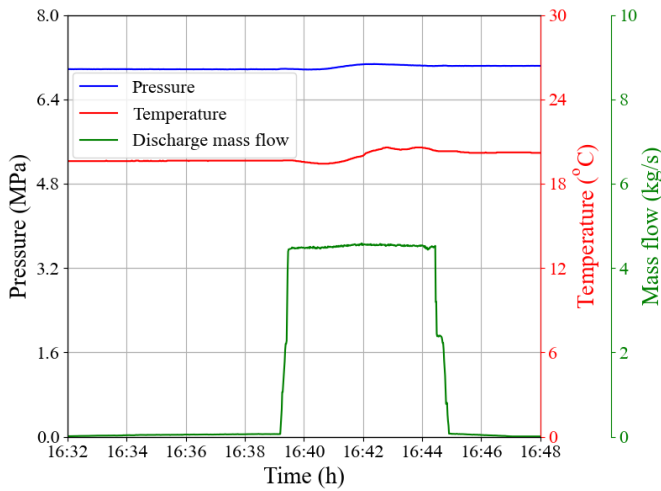
Fig. 2 Isobaric storage devices
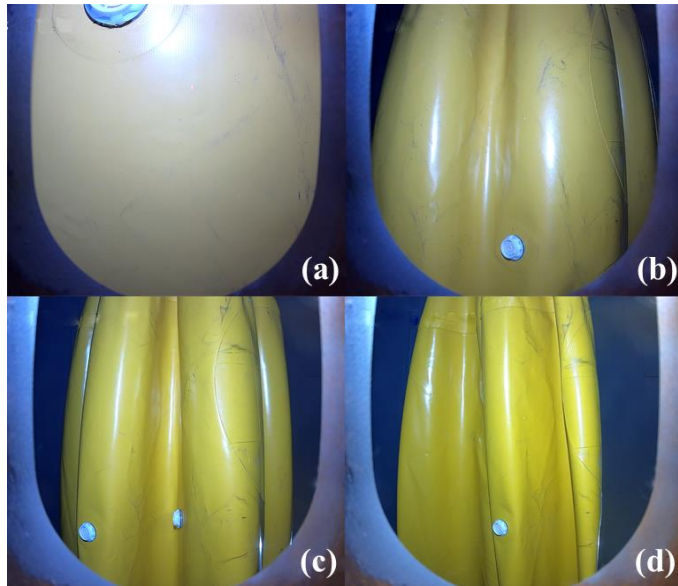
Fig. 3 Isobaric storage airbag

Three cameras were strategically positioned around the airbag to monitor the morphological changes of the flexible airbag. Fig. 3 depicts the alterations in the shape of the flexible air storage bag throughout the isobaric

energy discharge process. The figures illustrate that as the compressed air is discharged from the airbag, the airbag gradually diminishes in size (Fig. 3 (a)-(b)-(c)) until it is completely depleted (Fig. 3 (d)), indicating the complete release of compressed air. This is also one advantage of flexible isobaric air storage, allowing for maximizing gas storage space utilization. It can significantly reduce the construction expenses for gas storage.
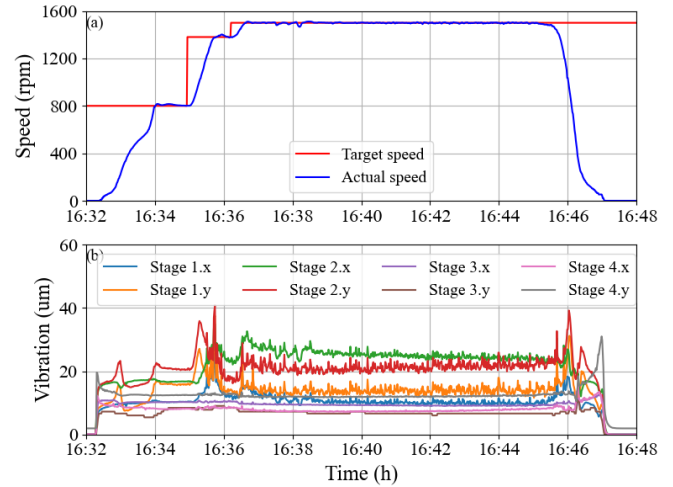
Fig. 4 Speed and vibration of turbine

The speed and vibration characteristics of the centripetal turbine during the experiment are presented in Fig. 4. Fig. 4(a) displays both the target speed and the actual speed of the turbine. The critical speed range of the centripetal turbine employed in this experiment spans from 900 rpm to 1150 rpm. Consequently, the target speeds of the centripetal turbine are set at 800 rpm, 1350 rpm, and 1500 rpm in sequence. Firstly, the no-load speed of the turbine is adjusted to 800 rpm to ensure the normal operation of the turbine and its auxiliary equipment. Then, the load is increased to approximately 400 kW by adjusting the turbine inlet pressure. Afterwards, the target speed is set to 1350 rpm to pass through the critical speed region. Subsequently, the load is increased to approximately 400 kW by adjusting the turbine inlet pressure once more. Finally, the speed is set to 1500 rpm, and the load is gradually increased to the rated load. The experimental results indicate that during the speed increase process, the speed overshoot does not exceed 15 rpm, and the fluctuation remains within 3 rpm after stabilization. Fig. 4 (b) displays the vibration characteristics in the X and Y directions of the turbine for all stages throughout the experiment. The vibration remains predominantly within 35 um, with the maximum value not exceeding 41 um. During the gas source switching process, there were no significant changes observed in the vibration of the

turbine. This indicates the stable and reliable mechanical performance of the turbine unit under all operational conditions.

The cold start from a standstill at 16:32:25 to 1500 rpm by 16:36:40 exhibited a remarkably swift duration of 4 minutes and 15 seconds, which is less than 5 minutes in total. The shutdown process is equally efficient, as the speed of the turbine decreases from 1500 rpm to a complete halt within 2 minutes. The energy discharge dynamics of the centripetal turbine indicate a load response time for the CAES of approximately 5 minutes, equivalent to the load response time of a pumped storage power station.
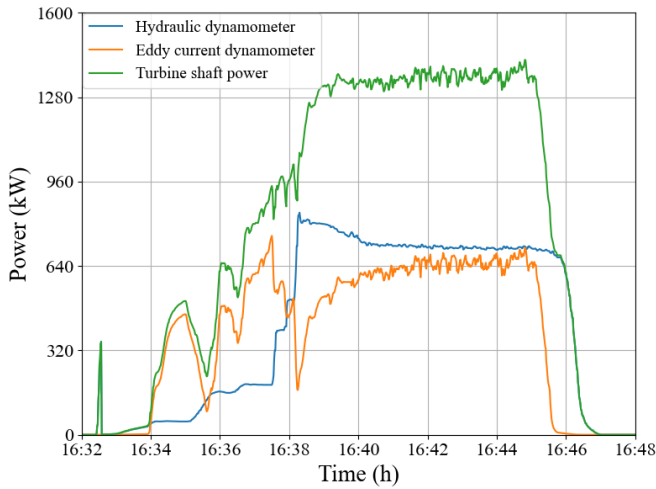
Fig. 5 Turbine shaft power varying with time

The variation of turbine shaft power over time is depicted in Fig. 5. Until 16:37:30, the water valve of the hydraulic dynamometer remained unchanged, stabilizing the turbine speed via the eddy current dynamometer. At 16:32, the target speed was set to 800 rpm, and the actual turbine speed gradually increased to 800 rpm. Subsequently, the load on the eddy current dynamometer was gradually increased from 0 to 457.42 kW by adjusting the turbine inlet pressure. At 16:35, the target speed was set to 1350 rpm while maintaining the turbine inlet pressure unchanged. The turbine speed quickly passed through the critical zone within 40 seconds, during which the power of the eddy current dynamometer decreased from 457.42 kW to 88.51 kW. The power of the eddy current dynamometer was increased to 489.63 kW by adjusting the turbine inlet pressure before setting the target speed to 1500 rpm. Subsequently, after setting the target speed to 1500 rpm and maintaining a constant turbine inlet pressure, the power of the eddy current dynamometer decreased from 489.63 kW to 347.60 kW. The power of the eddy current dynamometer was increased to 754.53 kW before the hydraulic dynamometer was engaged. From 16:37:30 to 16:38:10, the load of the eddy current dynamometer was gradually transferred to the hydraulic dynamometer by adjusting the water gate of the hydraulic dynamometer. Then, the turbine inlet pressure was gradually increased to raise the load of the eddy current dynamometer. Eventually, the combined load of the eddy current dynamometer and the hydraulic dynamometer reached 1352.90 kW. Throughout the gas source switching process, the total load remained relatively stable.

5. CONCLUSIONS

An experimental study on the discharge process of a megawatt isobaric compressed air energy storage system was conducted in this paper. The study reveals the startup, isobaric discharge operation, and shutdown characteristics of the energy storage system. It exhibits reliable and rapid regulation characteristics, with vibration less than 41um, cold start time not exceeding 5 min, and shut down within 2 min. The flexible air storage device can fully utilize the stored compressed air while maintaining stable pressure at the compressor outlet and turbine inlet. The turbine shaft power reaches 1352.90 kW. The research findings are expected to promote the widespread application of isobaric compressed air energy storage technology in coastal areas, supporting the large-scale utilization of renewable energy, and promoting sustainable development in coastal regions.

REFERENCE
[1] Chen Y, Xie H, Lu G, Zhang L, Yan J, Li S. Transient voltage stability assessment of renewable energy grid based on residual SDE-Net. Energy Reports. 2022;8:991-1001.
[2] Benyamina F, Ahmed H, Benrabah A, Khoucha F, Achour Y, Benbouzid M. Sequence extraction-based low voltage ride-through control of grid-connected renewable energy systems. Renewable and Sustainable Energy Reviews. 2023;183:113508.
[3] Saha S, Saleem MI, Roy TK. Impact of high penetration of renewable energy sources on grid frequency behaviour. International Journal of Electrical Power & Energy Systems. 2023;145:108701.
[4] Xu T, Gao W, Qian F, Li Y. The implementation limitation of variable renewable energies and its

impacts on the public power grid. Energy. 2022;239:121992.

[5] Huang ZF, Chen WD, Wan YD, Shao YL, Islam MR, Chua KJ. Techno-economic comparison of different energy storage configurations for renewable energy combined cooling heating and power system. Applied Energy. 2024;356:122340.

[6] Nasir J, Javed A, Ali M, Ullah K, Kazmi SAA. Capacity optimization of pumped storage hydropower and its impact on an integrated conventional hydropower plant operation. Applied Energy. 2022;323:119561.

[7] Sarmast S, Rouindej K, Fraser RA, Dusseault MB. Optimizing near-adiabatic compressed air energy storage (NA-CAES) systems: Sizing and design considerations. Applied Energy. 2024;357:122465.

[8] Yu S, Zhou S, Chen N. Multi-objective optimization of capacity and technology selection for provincial energy storage in China: The effects of peak-shifting and valley-filling. Applied Energy. 2024;355:122289.

[9] Li W, Yang T, Xin Y. New configuration to improve the power input/output quality of a superconducting energy storage/convertor. Journal of Energy Storage. 2023;68:107654.

[10] Dongxu H, Xingjian D, Wen L, Yangli Z, Xuehui Z, Haisheng C, et al. A review of flywheel energy storage rotor materials and structures. Journal of Energy Storage. 2023;74:109076.

[11] Shivani, Duddi R, Singh AK, Kamboj N, Kumar S. Enhancing the performance of Zn-ion capacitors with electrochemically tailored NiCo-LDH@Co3O4 nanoflakes on Ni foam. Journal of Energy Storage. 2024;91:112028.

[12] Chen H, Cong TN, Yang W, Tan C, Li Y, Ding Y. Progress in electrical energy storage system: A critical review. Progress in Natural Science. 2009;19:291-312.

[13] Ali S, Stewart RA, Sahin O, Vieira AS. Integrated GIS-AHP-based approach for off-river pumped hydro energy storage site selection. Applied Energy. 2023;337:120914.

[14] Jiang H, Yao L, Zhou C. Assessment of offshore wind-solar energy potentials and spatial layout optimization in mainland China. Ocean Engineering. 2023;287:115914.

[15] Alirahmi SM, Gundersen T, Arabkoohsar A, Klemeš JJ, Sin G, Yu H. Process design, integration, and optimization of a novel compressed air energy storage for the coproduction of electricity, cooling, and water. Renewable and Sustainable Energy Reviews. 2024;189:114034.

[16] Wang Z, Carriveau R, Ting DSK, Xiong W, Wang Z. A review of marine renewable energy storage. International Journal of Energy Research. 2019;43:6108-50.

[17] Liu C, Su X, Yin Z, Sheng Y, Zhou X, Xu Y, et al. Experimental study on the feasibility of isobaric compressed air energy storage as wind power side energy storage. Applied Energy. 2024;364:123129.

[18] Sun K, Liu M, Lu C, You Y, Zhang J, Meng W, et al. 2D design and characteristic analysis of an underwater airbag with mooring for underwater compressed air energy storage. Ocean Engineering. 2023;285:115515.

[19] Liu Z, Ding J, Huang X, Liu Z, Yan X, Liu X, et al. Analysis of a hybrid heat and underwater compressed air energy storage system used at coastal areas. Applied Energy. 2024;354:122142.

[20] Pottie D, Cardenas B, Garvey S, Rouse J, Hough E, Bagdanavicius A, et al. Comparative Analysis of Isochoric and Isobaric Adiabatic Compressed Air Energy Storage. Energies. 2023;16:2646.

[21] Pimm AJ, Garvey SD, de Jong M. Design and testing of Energy Bags for underwater compressed air energy storage. Energy. 2014;66:496-508.

[22] Bassett KP. Underwater Energy Storage - Emphasis on Buoyancy Technique. University of Windsor (Canada). 2017.

[23] Ebrahimi M, Carriveau R, Ting DSK, McGillis A. Conventional and advanced exergy analysis of a grid connected underwater compressed air energy storage facility. Applied Energy. 2019;242:1198-208.

[24] Neu T, Solliec C, dos Santos Piccoli B. Experimental study of convective heat transfer during liquid piston compressions applied to near isothermal underwater compressed-air energy storage. Journal of Energy Storage. 2020;32:101827.

[25] Neu T, Subrenat A. Experimental investigation of internal air flow during slow piston compression into isothermal compressed air energy storage. Journal of Energy Storage. 2021;38:102532.